Journal of Macromolecular Science, Part A
Publication details, including instructions for authors and subscription information:
http://www.informaworld.com/smpp/title~content=t713597274

Amorphous Thin Films of Chiral Binaphthyls for Photonic Waveguides

W. N. Herman[a]; Y. Kim[a]; W. L. Cao[a]; J. Goldhar[a]; C. H. Lee[a]; M. M. Green[b]; V. Jain[b]; M. -J. Lee[b]
[a] Laboratory for Physical Sciences, College Park, Maryland, USA [b] Herman F. Mark Polymer Research Institute, Polytechnic University, Brooklyn, New York, USA

Online publication date: 10 July 2003

To cite this Article Herman, W. N. , Kim, Y. , Cao, W. L. , Goldhar, J. , Lee, C. H. , Green, M. M. , Jain, V. and Lee, M. -J.(2003) 'Amorphous Thin Films of Chiral Binaphthyls for Photonic Waveguides', Journal of Macromolecular Science, Part A, 40: 12, 1369 — 1382
To link to this Article: DOI: 10.1081/MA-120025316
URL: http://dx.doi.org/10.1081/MA-120025316

JOURNAL OF MACROMOLECULAR SCIENCE®
Part A—Pure and Applied Chemistry
Vol. A40, No. 12, pp. 1369–1382, 2003

Amorphous Thin Films of Chiral Binaphthyls for Photonic Waveguides

W. N. Herman,[1,*] Y. Kim,[1] W. L. Cao,[1] J. Goldhar,[1] C. H. Lee,[1] M. M. Green,[2] V. Jain,[2] and M.-J. Lee[2]

[1]Laboratory for Physical Sciences, College Park, Maryland, USA
[2]Herman F. Mark Polymer Research Institute, Polytechnic University, Brooklyn, New York, USA

ABSTRACT

The synthesis of chiral nonracemic materials and the polarization properties of chiral optical waveguides fabricated from them are presented. These materials are based on binaphthyl compounds designed to produce a glassy isotropic optically active material in a thin solid film form. Chiral-core optical waveguides may find use as novel elements in integrated optic devices for photonics applications.

Key Words: Chiral; Amorphous glass; Binaphthyl; Waveguides; Photonics; Optical activity.

INTRODUCTION

Chiral macromolecules that form amorphous isotropic thin solid films have potential use in optical waveguides for photonics applications. Recent modeling results for asymmetric planar waveguides with chiral cores[1] suggests that novel optical device designs involving chiral materials may be possible, provided low loss amorphous films of

*Correspondence: W. N. Herman, Laboratory for Physical Sciences, 8050 Greenmead Drive, College Park, MD 20740, USA; Fax: 301-935-6723; E-mail: herman@lps.umd.edu.

DOI: 10.1081/MA-120025316
1060-1325 (Print); 1520-5738 (Online)

MARCEL DEKKER, INC.
270 Madison Avenue, New York, New York 10016

sufficient chirality[2] can be fabricated. Potential applications include passive transverse electric (TE)–transverse magnetic (TM) mode converters for rotating the polarization of the output of semiconductor lasers to optimize the polarization for downstream active waveguide devices in integrated optics, conversion of linear polarization to and from elliptical polarization, and active polarization control by combining an optically active waveguide segment with an electro-optic phase shifter. There is a distinct advantage to achieving polarization rotation by optical activity instead of linear birefringence. For a birefringent linear polarization rotator, the input polarization must be at a 45° angle to the optic axis—a condition which is difficult to achieve in integrated optics. An optically active bulk material that is isotropic, on the other hand, will rotate a linearly polarized input of any orientation to a linearly polarized output.[3] To make use of this advantage in integrated optics, the chiral waveguide modes must be circularly polarized.

The challenge for this application is to synthesize macromolecular structures with a high degree of chirality, ultimately extending into the near infrared, that also form amorphous isotropic thin films with negligible linear birefringence. Large specific rotations on the order of 15,000 deg $cm^3/(dm\,g)$ have been realized, for example, with helicenes.[4,5] However, these molecules tend to aggregate in the formation of thin films, a feature which can cause increased optical loss.

In this paper, we present progress in the development of chiral-core optical waveguides from amorphous organic materials. Although there has been relatively recent interest in the nonlinear optical properties of chiral materials,[6–10] here we focus on the linear optical effects of chirality on the modes in waveguides fabricated from chiral materials. We first summarize some properties of modes in chiral waveguides, then present the synthesis of enantiomeric binaphthyl molecular structures designed to promote isotropy (i.e., absence of linear birefringence) in thin solid films, and finally present the fabrication process for and optical characterization of slab waveguides made from these materials.

Chiral Optical Waveguides

The polarization ellipticity of the modes of light propagating in chiral core waveguides depends in part on a material chirality parameter γ, which appears in the constitutive equations adjunct to Maxwell's equations.[1] This parameter is related to the bulk rotatory power ρ through:

$$\rho = k_0{}^2 n_g{}^2 \gamma, \quad k_0 = \frac{2\pi}{\lambda}, \quad \text{and} \quad n_g = \sqrt{\frac{\varepsilon}{\varepsilon_0}} \tag{1}$$

where n_g is the average refractive index and ε is the permittivity. For reference, a chirality parameter value of $\gamma = 1$ picometer corresponds to a bulk rotatory power $\rho = 15°/\text{mm}$ at a wavelength of 633 nm and average refractive index 1.62. The ellipticity of the modes also depends on the waveguide structure and relative values of the core and cladding indices as discussed below.

We are concerned here with a slab waveguide structure, i.e., a planar core sandwiched between upper and lower cladding materials having refractive indices n_0 and n_s, respectively, with $n_g > n_0$ and $n_g > n_s$. For an achiral core, it is well known that the optical modes are TE and TM. Using the theory presented in Ref. [1], an example of the transition

Marcel Dekker, Inc.
270 Madison Avenue, New York, New York 10016

with increasing chirality from TE/TM modes in the achiral case to predominantly right- and left-handed circularly polarized (RHC/LHC) modes is illustrated in Fig. 1 for two different 3 μm thick planar waveguides, one asymmetric and the other symmetric, both with an average core index of $n_g = 1.62$. The dotted lines correspond to an asymmetric waveguide with upper and lower cladding refractive indices of 1.00 and 1.615, respectively, and the solid lines correspond to a symmetric waveguide having upper and lower cladding indices of 1.615. The parameter g is proportional to the ellipticity of the polarization ellipse (ratio of E_x to E_y for the transverse optical electric field) and is plotted vs. the chirality parameter γ for the lowest order elliptical modes supported by this waveguide. For increasing chirality γ, the top half of the plot ($g > 0$) shows the modes that are right-handed elliptical (RHE) evolving from TM modes at $\gamma = 0$, and the bottom half of the plot ($1/g < 0$) shows the modes that are left-handed elliptical (LHE) evolving from TE modes at $\gamma = 0$. The curves are labeled according to the handedness and mode number. The horizontal dotted lines identify the values $g = +1$ and $g = -1$ corresponding to RHC and LHC polarization, respectively.

From this plot, it is evident that we must have a material with $\gamma > 20$ pm (bulk $\rho = 300^\circ/\text{mm}$) in order to achieve nearly circularly polarized modes in an asymmetric planar waveguide where the top cladding is air. In the symmetric waveguide, however, circularly polarized modes can be obtained with considerably lower chirality, viz., $\gamma \approx 3$–4 pm (bulk $\rho = 45$–$60^\circ/\text{mm}$). The desire for circularly polarized modes, rather than just elliptically polarized modes, is driven by the goal of achieving a pure polarization

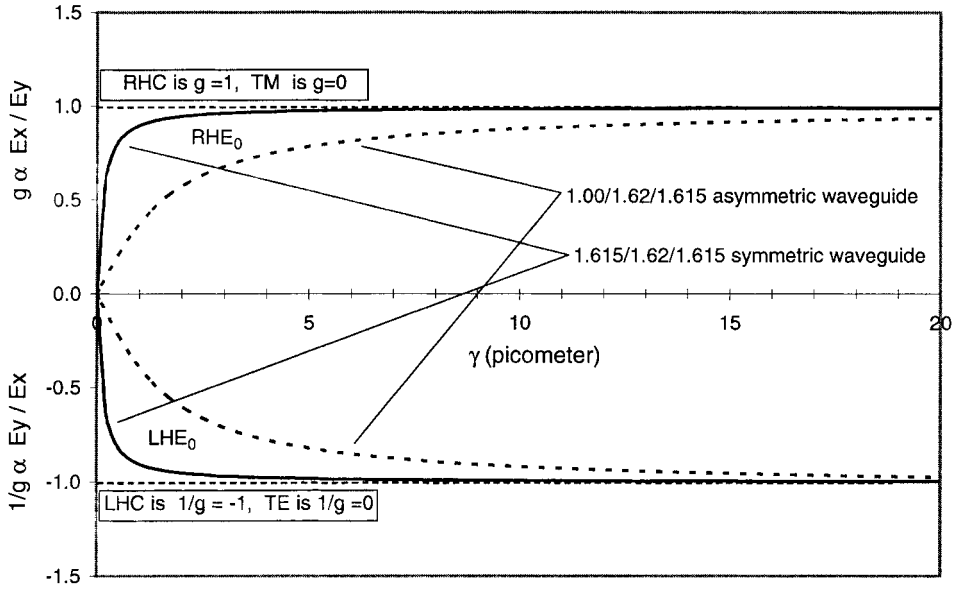

Figure 1. Plots of the ellipticity parameter g vs. chirality γ for the lowest order elliptical modes in a planar chiral-core waveguide. The solid lines are associated with a symmetric waveguide with refractive indices $n_g = 1.62$, $n_0 = n_s = 1.615$ and the dotted lines with an asymmetric waveguide having indices $n_g = 1.62$, $n_0 = 1.00$, $n_s = 1.615$.

rotator, i.e., a device for which a linearly polarized input is rotated to some other linearly polarized state for any propagation length. Because even moderate amounts of linear birefringence can overpower the effects of optical activity,[11] an essential requirement that must be fulfilled in order to attain this goal is the synthesis of a chiral material that is isotropic in a solid film. A scheme for designing such a material with negligible linear birefringence is presented in the next section and outlined in Fig. 2. The resulting optical rotatory dispersion is shown in Fig. 3. The method for insuring an isotropic material follows on the work of Shaw Chen who developed these glass forming methods.[12,13]

EXPERIMENTAL

^{1}H and ^{13}C NMR spectra were recorded on a Bruker DPX-300, the shifts are reported in δ (ppm) relative to tetraethyl silane as an internal standard. Circular dichroism (CD) and UV-VIS spectra were recorded on a JASCO J-710 Spectrophotometer and Cary 50 bio UV-VIS spectrophotometer. Optical rotation was measured on a JASCO P1010 polarimeter. Glass transition temperatures were recorded on a Perkin Elmer DSC7 series with a heating rate 10°C/min under nitrogen flow. Melting points were measured either on a Perkin Elmer DSC7 or on a Thomas capillary melting point apparatus.

For thin solid films, the refractive index dispersion of these films was measured using a Metricon™ prism coupler, which determines the ordinary and extraordinary index dispersion of a film using two orthogonal linear polarizations at each of five discrete laser wavelengths. The optical activity of the solid films was measured using a 670 nm laser with the laser beam passing through the film at normal incidence. For these films, normal incidence corresponds to propagation along the optic axis, and therefore, the circular birefringence can be measured independently of linear birefringence effects. The sample films were placed between two Glan-Thompson polarizers in a polarizer–analyzer configuration, and the analyzer was rotated about the null position using a computer-controlled precision rotation stage. From a fit of the data to a sine-squared curve, the change in the null position of the film on a fused quartz substrate was compared to the null for transmission through the substrate alone.

SYNTHESIS OF CHIRAL BINAPHTHYLS FORMING ISOTROPIC THIN FILMS

Materials

All the solvents were obtained from commercial sources and used without further purification, unless otherwise noted. THF and diethyl ether were distilled under nitrogen from Na/benzophenone. Acetone was dried over calcium chloride. Silica (70–230 mesh Astm) and tlc plates were purchased from Merck. *n*-BuLi (1.6 M in hexane) was purchased from Aldrich Chemical Company.

Dichloro-*bis*1,3(diphenylphosphino propane)nickel (II), tetrakis(triphenylphosphine)-palladium ($Pd(PPh_3)_4$), and trimethyl borate were purchased form Aldrich. *Trans*-1,3,5-cyclohexanetricarboxylic acid was prepared by the procedure reported by Steiz,[14] to convert commercially available *cis*-1,3,5-cyclohexane tricarboxylicacid into a *trans*

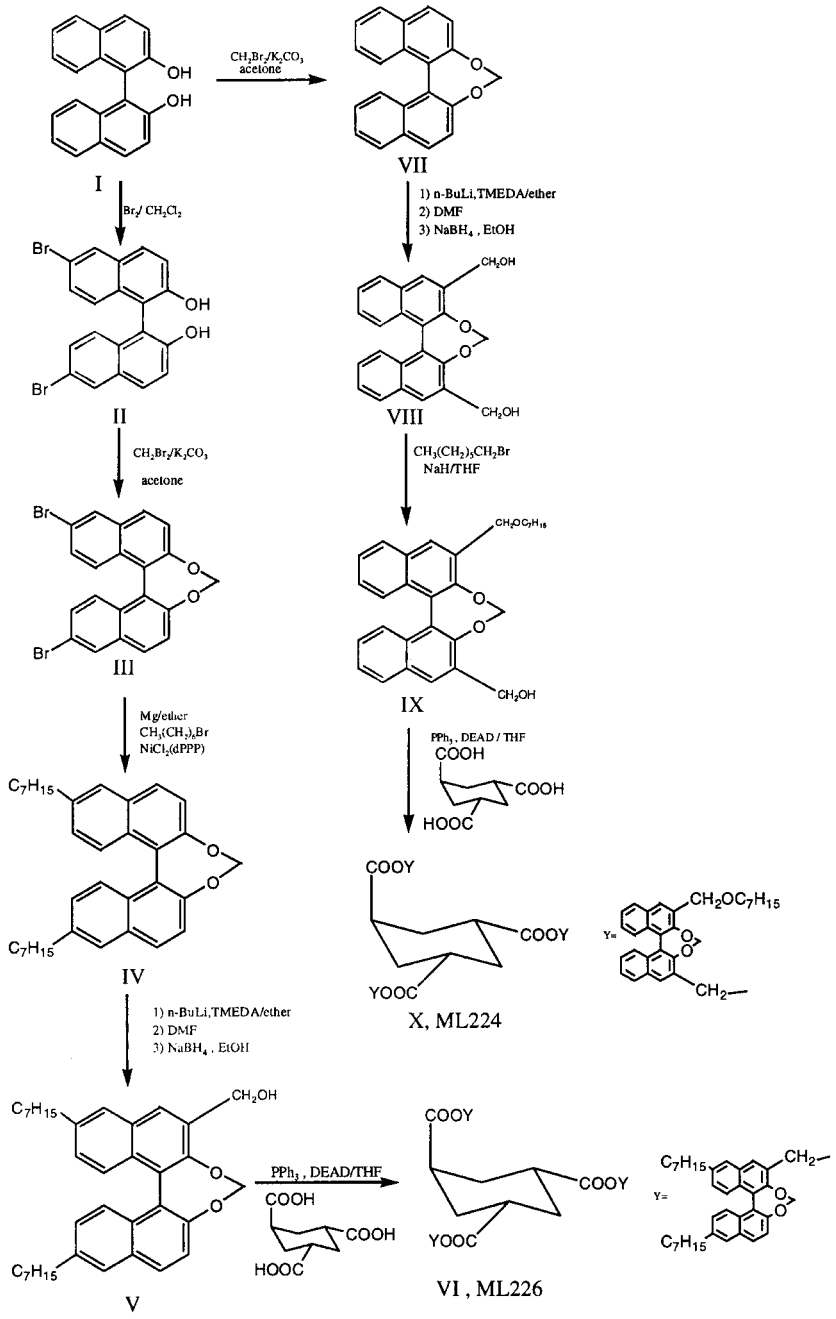

Figure 2. Outline of the synthesis of glass forming isotropic binaphthyl based chiral nonracemic compounds.

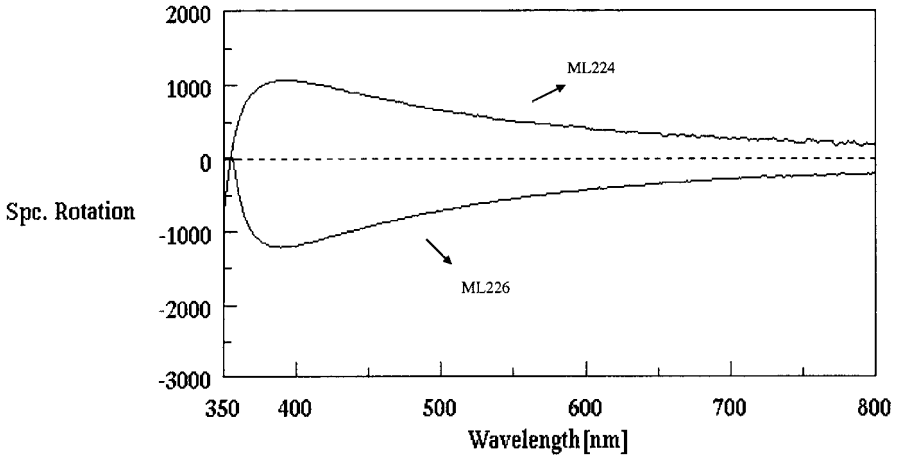

Figure 3. Optical rotatory dispersion spectra for ML226 (0.1% solution in CH_3CN, 0.1 cm path length) and ML224 (0.012% solution in $CHCl_3$, 0.1 cm path length).

isomer with a 1-axial 2-equtorial configuration. 1,1′-bi-2naphthol was synthesized and resolved by known methods[15] to yield (*R*)-1,1′-bi-2-naphthol in 99%ee $[\alpha]_D^{25} = -33.5^\circ$ (THF, 4 mg/mL) and the other enantiomer in 98%ee $[\alpha]_D^{25} = +34.3^\circ$ (THF, 10 mg/mL). The *R* enantiomer was used as the starting material for ML226(VI) and the *S* enantiomers was used for synthesizing ML224(X). (*S*)-1,1′-binaphthyl-2,2′diloxymethane (BNO,VII), (*R*)-6,6′-dibromo-1,1′-bi-2naphthol(II), and (*R*)-6,6′-dibromo-1,1′binaphthyl-2,2′diyloxymethane(III) were synthesized from the respective enantiomers of 1,1′-bi-2-naphthol following the known methods.[16]

(*R*)-(6,6′-Diheptyl-1,1′-binaphthyl-2,2′-diyloxy)Methane BNO (IV)

Mg turnings (0.7 g) and dry ethyl ether (5 mL) were placed in a three-neck 500 mL round bottom flask equipped with a dropping funnel and a reflux condenser. The dropping funnel was charged with 1-bromoheptane (3.2 g, 19.4 mmol) in dry ether (20 mL). The Grignard reaction was started by the addition of iodine crystals, and a few drops of 1-bromoheptane. As the color of iodine disappeared, the addition of bromoheptane solution was started and a dropping rate was adjusted to maintain a gentle reflux for 1 hr. After cooling, this Grignard solution was transferred via a cannula to another three-neck 250 mL flask containing 6,6′-dibromo BNO (3.12 g, 6.71 mmol) and $NiCl_2$ (dPPP) (0.42 g) in diethyl ether (50 mL) with rapid stirring at ice bath temperature. The mixture was slowly warmed to room temperature and stirred for 4 h. Water (100 mL) and 10% sulfuric acid (100 mL) were successively added to the mixture. The organic layer was separated, washed with water twice, and evaporated to dryness. The solid residue was purified by flash chromatography using ethyl acetate/hexane (1 : 4) as the eluent to yield 2.2 g of an yellow oily product (67%). $[\alpha]_D^{25} = -470^\circ$ (chloroform).

(*R*)-(−) 6,6′-Diheptyl-1,1′-binaphthyl-3-hydroxymethyl BNO (V)

(*R*)-(6,6′-diheptyl-1,1′-binaphthyl-2,2′-diyloxy)methane BNO (1.2 g, 2.57 mmol) was dissolved in a mixture of distilled diethyl ether (40 mL) and TMEDA (10 mL) under argon atmosphere for 30 min. *n*-BuLi (3.54 mL, 5.66 mmol was then added dropwise and the reaction mixture was stirred for 5 hr at room temperature. Freshly distilled DMF (0.52 mL, 6.7 mmol)was added to the reaction mixture and stirred overnight and then was poured into water (100 mL) and the flask rinsed with ethyl acetate (10 mL) twice. The resulting mixture was separated with ethyl acetate and washed with water. After drying with magnesium sulfate followed by filtration, the solvent was evaporated. The light yellow solid was used in the next reduction step without further purification.

A solution was prepared by dissolving the crude product and sodium borohydride (0.146 g) in 99% ethanol (50 mL) at room temperature. After stirring for 3 h the volume of the reaction mixture was reduced to 5 mL, which was shaken with 100 mL ethyl acetate and 70 mL of water. Upon removing the solvent from the organic layer by evaporation in vacuo, the solid residue was purified by flash column chromatography using ethyl acetate (1 : 2) as eluent to yield 0.52 g of the desired product. $[\alpha]_D^{25} = -452.8^\circ$ ($CHCl_3$).

ML226(VI)

To a stirred solution containing (*R*)-(−) 6,6′ diheptyl-1,1′-binaphthyl-3-hydroxymethyl BNO (0.45 g, 0.86 mmol), triphenylphosphine (0.29 g, 1.12 mmol), and *trans*-1,3,5-cyclohexanetricarboxylic acid (0.058 g, 0.27 mmol) in dry THF (20 mL) was added diethylazodicarboxylate (DEAD, 0.22 g, 1.3 mmol) dropwise, and the reaction mixture stirred for 5 h. After evaporation in vacuo to dryness, the crude product was purified by flash chromatography using ethyl acetate/hexane (1 : 5) as eluent (repeated twice) to yield 0.34 g of a colorless glassy product. $[\alpha]_D^{25} = -485^\circ$ ($CHCl_3$), $T_g = 57^\circ$C.

^{1}H NMR (300 MHz, $CDCl_3$): 7.80–7.94 (m, 6H), 7.62 (s, 6H), 7.27–7.43 (m, 9H), 7.09–7.20 (m, 6H), 5.59–5.70 (m, 6H), 5.28–5.49 (m, 6H), 3.02 (s, 1H), 2.65–2.82 (m, 14H), 2.38–2.57 (m, 3H), 1.61–1.76 (m, 14H), 1.22–140 (m, 48H), 0.89 (t, 18H).

^{13}C NMR (300 MHz, $CDCl_3$): 174.3, 173.7, 150.6, 148.8, 140.1, 139.9, 139.5, 132.0, 131.4, 130.7, 130.5, 129.9, 129.7, 128.1, 127.7, 127.5, 126.5, 126.4, 125.9, 120.7, 119.4, 103.1, 62.7, 38.0, 35.8, 31.7, 31.2, 29.7, 29.4, 29.2, 29.0, 22.7, 22.6, 14.1.

(*S*) (+)-3,3′ Dihydroxymethyl BNO (VIII)

(*S*)-1,1′-binaphthyl-2,2′diyloxymethane (VII) (1.00 g, 3.39 mmol) was dissolved in a mixture of distilled diethylether 50 mL and TMEDA 10 mL under argon atmosphere for 30 min. *n*-BuLi (7.3 mL, 11.9 mmol) was then added dropwise and the reaction mixture was stirred for 5 h at room temperature. Freshly distilled DMF (1.4 mL, 14.3 mmol) was added to the reaction mixture and stirred overnight. It was poured into water (100 mL) and the flask was rinsed with ethyl acetate (100 mL) twice. The resulting mixture was separated with ethyl acetate and washed with water. After drying with magnesium sulfate followed by filtration, the solvent was evaporated. The light yellow solid obtained was used in the next step without purification.

A solution was prepared by dissolving the crude product and sodium borohydride (0.12 g, 3.07 mmol) in 99% ethanol (80 mL) at room temperature. After stirring for 3 h, the volume of the reaction mixture was reduced to 5 mL, which was shaken with 100 mL ethyl acetate and 70 mL water. Upon removing the solvent from organic layer by evaporation in vacuum, the solid residue was purified by flash column chromatography using ethyl acetate/hexane (1 : 1) as the eluent to yield 0.90 g of a white powder. MP 218°C, $[\alpha]_D^{25} = +551$ ($CHCl_3$).

(*S*)-(+)-3-Heptyloxymethyl-3′-hydroxymethyl BNO (IX)

To a mixture of (*S*)-(+)-3,3′-dihydroxymethyl BNO (0.95 g, 2.51 mmol) and sodium hydride (0.24 g, 10.3 mmol) in dry THF (70 mL) was added 1-bromoheptane (0.67 g, 3.85 mmol) under an argon atmosphere. The reaction mixture was refluxed for 2 days. The solvent was removed in vacuum and the crude product was purified by flash column chromatography using ethyl acetate/hexane (1 : 5) as eluent to yield 0.45 g of a white solid. MP 199°C, $[\alpha]_D^{25} = +543$ ($CHCl_3$).

ML224(X)

To a stirred solution containing (*S*)-(+)-3-heptyloxymethyl-3′-hydroxymethyl BNO (IX) (0.48 g), triphenylphosphine (0.375 g) and *trans*-1,3,5-cyclohexanetricarboxylic acid (0.06 g) in dry THF 20 mL was added DEAD, 0.31 g,) drop wise, and the reaction mixture stirred for 5 h. After evaporation in vacuum to dryness, the crude product was purified by flash chromatography using ethyl acetate/hexane (1 : 5) as eluent (repeated twice) to yield 0.3 g of a colorless glassy product $[\alpha]_D^{25} = +415.6$ ($CHCl_3$), $T_g = 56$°C.

^{1}H NMR(300 MHz, $CDCl_3$): 7.80–8.07 (m, 12H), 7.23–7.46 (m, 18H), 5.71 (d, 6H), 5.32–5.50 (m, 6H), 4.88 (dd, 3H), 4.63 (dd, 3H), 3.59 (t, 6H), 3.07 (s, 1H), 2.81 (t, 2H), 2.40–2.54 (m, 3H), 2.36–2.54 (m, 3H), 1.60–1.78 (m, 8H), 1.21–1.42 (m, 25H), 0.87 (t, 9H).

^{13}C NMR (300 MHz, $CDCl_3$): 173.2, 172.8, 148.3, 148.1, 131.1, 130.7, 130.4, 130.2, 129.3, 127.4, 126.7, 125.7, 125.3, 125.0, 124.9, 124.2, 102.1, 69.9, 67.6, 61.4, 59.3, 37.2, 30.8, 28.8, 28.2, 25.2, 21.6, 13.1.

Waveguide Fabrication

Asymmetric slab waveguides were fabricated from ML224 and ML226 on a SiON layer deposited on a GaAs substrate as shown in Fig. 4. The refractive index of the SiON layer was adjusted to be close to that of the chiral-core layer by controlling the ratio of gas mixture in PECVD. A small index difference between the core and the cladding layer is desirable because it can enhance the ellipticity of the modes for a given amount of material chirality.[1] A solution of ML224 and ML226 dissolved in cyclohexanone (~27% by weight) was spin-coated at 1000 rpm for 30 s on SiON to achieve approximately 3 μm thick films, and then cured at around T_g in a N_2 oven. For the final step, the waveguides were cleaved to form a smooth end facet.

Marcel Dekker, Inc.
270 Madison Avenue, New York, New York 10016

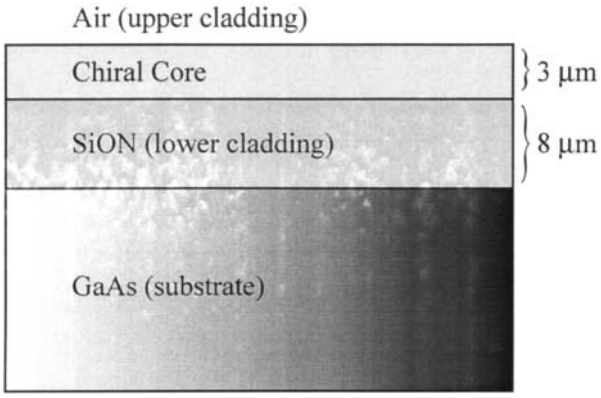

Figure 4. Structure of chiral slab waveguides spun on GaAs substrates coated with silicon oxynitride.

RESULTS AND DISCUSSION

The linear refractive index of the binaphthyl films fabricated from ML224 and ML226 was isotropic within the experimental measurement uncertainty of ± 0.0001, as shown in Fig. 5. For binaphthyl films fabricated from ML224 and ML226 in fused quartz substrates, earlier, we reported rotatory powers of $+5.7^\circ$/mm, and -3.3°/mm, respectively.[17] These are consistent with the specific rotatory powers measured in solution.

The state of polarization (SOP) of the modes in these thin film asymmetric waveguides was characterized by determining normalized Stokes parameters[18] of the

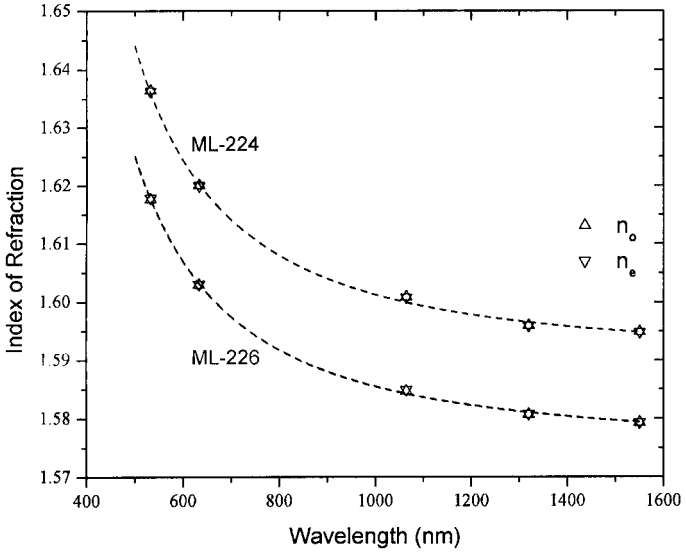

Figure 5. Linear refractive index dispersion of ML224 and ML226.

light output of the waveguides corresponding to each of two orthogonal input linear polarizations. We refer to these orthogonal linearly polarized inputs as TE and TM because in an achiral film they would excite the usual TE and TM modes. For chiral waveguides, a linearly polarized input will excite both eigenmodes, RHE and LHE, and the TE input excites a different relative fraction of these elliptical eigenmodes than the TM input. As the light propagates down the waveguide, the RHE and LHE modes travel at different speeds resulting in an overall elliptical polarization with a rotated major axis at the output of the waveguide. (If the eigenmodes are circular, the output polarization is a rotated linear polarization.) By determining the output polarization state for a given input state, the eigenmodes of the slab waveguide can be determined. This process is described in more detail below for slab waveguides fabricated from ML224 and ML226.

The Stokes parameters corresponding to a transverse electric field:

$$E_T = \begin{pmatrix} A_x \exp(i\delta_x) \\ A_y \exp(i\delta_y) \end{pmatrix} \tag{2}$$

are defined by:[18]

$$S_0 = {A_x}^2 + {A_y}^2, \quad S_1 = {A_x}^2 - {A_y}^2, \quad S_2 = 2A_xA_y\cos(\delta), \quad S_3 = 2A_xA_y\sin(\delta) \tag{3}$$

where $\delta = \delta_y - \delta_x$. The experimental setup is shown in Fig. 6. The detector measures the intensity from the output of the waveguide after additionally propagating through a single mode fiber. The SOP of the light output from the fiber is determined using a rotating quarter waveplate and linear polarizer. The light output power from the fiber is measured as

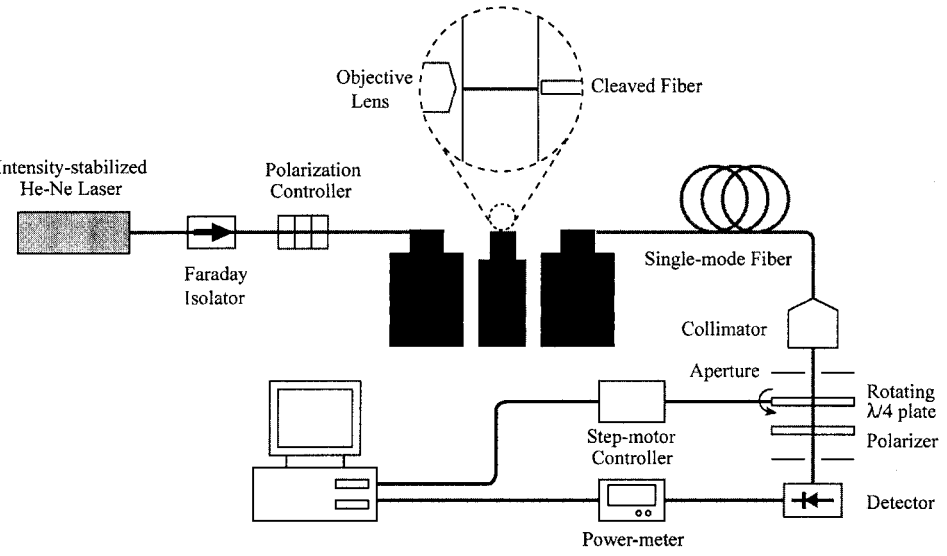

Figure 6. Experimental setup for characterization of the polarization states of the modes in thin film planar waveguides.

a function of the angle θ of the fast axis of a quarter waveplate rotating with respect to the transmission axis of a fixed linear polarizer. This angular dependence is given by Ref.[19].

$$P(\theta, S) = \frac{1}{4}S_0 + \frac{1}{4}(\cos^2 2\theta)S_1 + \frac{1}{8}(\sin 4\theta)S_2 - \frac{1}{4}(\sin 2\theta)S_3 \tag{4}$$

The Stokes parameters of the signal at the output of the fiber are then obtained by a linear fit to this equation. The collected data along with a fit to Eq. (4) for slab waveguides of ML224 and ML226 is given in Fig. 7.

In order to determine the SOP at the output of the waveguide, the polarization effects of the fiber must be accounted for. This can be done by a calibration process in which three different input polarizations, $(S_1, S_2, S_3) = (1,0,0)$, $(0,-1,0)$, and $(0,0,1)$, representing horizontal linear polarization, -45° linear polarization and RHC polarization, respectively, are launched into the fiber and the resulting output SOP for each case is determined as above.[20] The calibration determines a characteristic 3×3 Mueller matrix M[21] that determines the SOP at the output of the fiber for a given input state. The M matrix can then be inverted to determine the SOP at the input of the fiber (and thus the output of the chiral waveguide) when the SOP at the output is known.

The Stokes parameters describing the eigenstates of the waveguide are determined from the SOP at the waveguide output using the property that the continuous evolution of the polarization states from initial SOP to final SOP while the light propagates through the waveguide is a rotation about an axis connecting orthogonal eigenstates on the Poincare sphere.[18] For ML224 we obtain the elliptical eigenstates:

$$\begin{pmatrix} S_1 \\ S_2 \\ S_3 \end{pmatrix}_{\substack{\text{eigen modes} \\ \text{from TM input}}} = \pm \begin{pmatrix} -0.88 \\ 0 \\ 0.47 \end{pmatrix}, \quad \begin{pmatrix} S_1 \\ S_2 \\ S_3 \end{pmatrix}_{\substack{\text{eigen modes} \\ \text{from TE input}}} = \pm \begin{pmatrix} 0.90 \\ 0 \\ -0.44 \end{pmatrix} \tag{5}$$

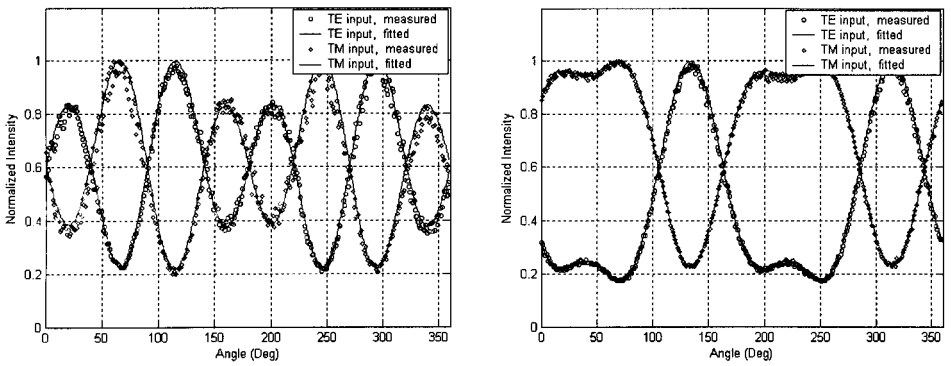

(a) ML224 (b) ML226

Figure 7. Detected optical power as a function of rotating quarter waveplate orientation for determining the Stokes parameters characterizing the polarization of the waveguide modes. The solid lines fit to Eq. (4) for slab waveguides fabricated from (a) ML224 and (b) ML226.

and for ML226

$$\begin{pmatrix} S_1 \\ S_2 \\ S_3 \end{pmatrix}_{\substack{\text{eigen modes} \\ \text{from TM input}}} = \pm \begin{pmatrix} 0.88 \\ 0 \\ 0.48 \end{pmatrix}, \quad \begin{pmatrix} S_1 \\ S_2 \\ S_3 \end{pmatrix}_{\substack{\text{eigen modes} \\ \text{from TE input}}} = \pm \begin{pmatrix} -0.88 \\ 0 \\ -0.47 \end{pmatrix} \tag{6}$$

The ellipticities g of the eigenstates can be deduced from the S_3 values using the relation

$$S_3 = \frac{2g}{1+g^2} \tag{7}$$

For both ML224 and ML226, the eigenmodes have ellipticities of approximately 0.25, which is consistent with that expected from a chiral material with $\gamma \approx 0.3$–0.4 pm (see Fig. 1).

CONCLUSION

Binaphthyl based chiral nonracemic compounds, identified as ML224 and ML226, have been synthesized using a scheme designed to produce materials that form glassy isotropic thin solid films with negligible linear birefringence. Thin solid films of these materials were fabricated and evaluated for potential use as the guiding layer in chiral core waveguides, which have potential use for polarization control in integrated optics applications. Refractive index measurements indicated that the films were quite isotropic—any linear birefringence present was less than the experimental error of ± 0.0001. The specific rotation measured in solution was $[\alpha]_D^{25} = +415.6^\circ$ for ML224 and $[\alpha]_D^{25} = -485^\circ$ for ML226. The corresponding rotatory power measured at a wavelength of 670 nm for the thin solid films was less than 6°/mm in magnitude for both materials. Detailed experimental polarization analysis was carried out on the modes in asymmetric planar waveguide structures fabricated on silicon oxynitride buffer layers deposited on GaAs wafers with the chiral binaphthyl material as the core. This analysis indicated that the modes for the chiral waveguides were indeed elliptically polarized. Ellipticities (ratio of E_x to E_y for the optical transverse electric field) on the order of 0.25 were achieved. Theory indicates that symmetric waveguides of these same materials could yield ellipticities of 0.75. This work demonstrates that isotropic chiral materials can be designed and synthesized for the fabrication of optical waveguides having elliptical modes. In order to obtain modes that are circularly polarized, as desired for an integrated optic polarization rotator, it is estimated that isotropic materials with specific rotations about a factor of 10 higher than those achieved here are needed. In addition, it is desirable to extend the optical rotatory dispersion (ORD) maxima towards the infrared for telecommunications applications. The design and synthesis of such materials is in progress.

ACKNOWLEDGMENTS

Financial support by the Office of Naval Research for both the Laboratory for Physical Sciences and the Polytechnic University is gratefully acknowledged. In addition, the

research at the Polytechnic University is also supported by the National Science Foundation and the Petroleum Research Fund, administered by the American Chemical Society.

REFERENCES

1. Herman, W.N. Polarization eccentricity of the transverse field for modes in chiral core planar waveguides. J. Opt. Soc. Am. A **2001**, *18* (11), 2806–2818.
2. For reviews of macromolecular chirality, see Green, M.M.; Park, J.-W.; Sato, T.; Lifson, S.; Selinger, R.L.B.; Selinger, J.V. Angew. Chem. Int. Ed. **1999**, *38*, 3138; Nakano, T.; Okamoto, Y. Synthetic helical polymers: conformation and function. Chem. Rev. **2001**, *101*, 4013–4038.
3. See, for example, Salah, B.E.A.H.; Teich, M.C. Polarization and crystal optics. In *Fundamentals of Photonics*; John Wiley and Sons: New York, 1991; Chap. 6.
4. Nuckolls, C.; Katz, T.J.; Katz, G.; Collings, P.J.; Castellanos, L. Synthesis and aggregation of a conjugated helical molecule. J. Am. Chem. Soc. **1999**, *121*, 79.
5. Lovinger, A.J.; Nuckolls, C.; Katz, T.J. Structure and morphology of helicene fibers. J. Am. Chem. Soc. **1998**, *120*, 264–268.
6. Elshocht, S.V.; Verbiest, T.; Kauranen, M.; Persoons, A.; Langeveld-Voss, B.M.W.; Meijer, E.W. Direct evidence of the failure of electric-dipole approximation in second harmonic generation from a chiral polymer film. J. Chem. Phys. **1997**, *107* (19), 8201–8203.
7. Verbiest, T.; Elshocht, S.V.; Kauranen, M.; Hellemans, L.; Snauwaert, J.; Nuckolls, C.; Katz, T.J.; Persoons, A. Strong enhancement of nonlinear optical properties through supramolecular chirality. Science **1998**, *282*, 913–915.
8. Ostroverkhov, V.; Ostroverkhova, O.; Petschek, R.G.; Singer, K.D.; Sukhomlinova, L.; Twieg, R.J. Prospects for chiral nonlinear optical media. IEEE J. on Selected Topics in Quantum Electronics **2001**, *7* (5), 781–792.
9. Ostroverkhov, V.; Singer, K.D.; Petschek, R.G. Second-harmonic generation in nonpolar chiral materials: relationship between molecular and macroscopic properties. J. Opt. Soc. Am. B **2001**, *18* (12), 1858–1865.
10. Han, S.H.; Wu, J.W.; Kang, J.-W.; Shin, Y.-D.; Lee, J.-S.; Kim, J.-J. Induced chirality in a polyisocyanate polymeric film and the change in polarization rotation under an external electric field. J. Opt. Soc. Am. B **2001**, *18* (3), 298–301.
11. Nye, J.F. *Physical Properties of Crystals*; Oxford University Press: Oxford, Great Britain, 1957; Chap. 14.
12. Shi, H.; Chen, S.H. Novel glass forming liquid crystals II systems containing 1-phenyl-2-(6-cyanonaphth-2-yl)ethyne as ahigh optical birefringence moiety. Liq. Cryst. **1995**, *18*, 733–741.
13. Fan, F.F.; Mastrangelo, J.C.; Katsis, D.; Chen, S.H. Novel glass forming liquid crystals V. Nematic and chiral-nematic systems with an elevated glass transition temperature. Liq. Cryst. **2000**, *27*, 1239–1248.
14. Steitz, A., Jr. Epimers of 1,3,5-cyclohexanetricarboxylic acid. Org. Chem. **1968**, *33*, 2978.
15. Park, J.W.; Ediger, M.D.; Green, M.M. Chiral studies in amorphous solids: the effect of the polymeric glassy state on the racemization kinetics of bridged paddled binaphthyls. J. Am. Chem. Soc. **2001**, *123*, 49.

16. (a) Sogah, G.D.Y.; Cram, D.J. Host-guest complexation. Host covalently bound to polystyrene resin for chromatographic resolution of enantiomers of amino acids and ester salts. J. Am. Chem. Soc. **1979**, *101*, 3035; (b) Deussen, H.J.; Hendrickx, E.; Boutton, C.; Krog, D.; Clays, K.; Bechgaard, K.; Persoons, A.; Bjørnholm, T. Novel chiral bis dipolar 6,6′-disubstituted binaphthol derivatives for second order non linear optics: synthesis and linear and non linear optical properties. J. Am. Chem. Soc. **1996**, *118*, 6841.
17. Kim, Y.; Cao, W.; Goldhar, J.; Lee, C.H.; Herman, W.N. Optical waveguides from amorphous chiral binaphthyl films. Polymer Preprints **2002**, *43* (2), 595.
18. Huard, S. *Polarization of Light*; J. Wiley and Sons: Chichester, UK, 1997; Chap. 1.
19. Collette, E. Ed. *Polarized Light: Fundamentals and Applications*; Marcel Dekker Inc.: New York, 1993; 103 pp.
20. Van Wiggeren, G.D.; Roy, R. High-speed fiber-optic polarization analyzer, measurements of the polarization dynamics of an erbium-doped fiber ring laser. Opt. Comm. **1999**, *164*, 107–120.
21. Tang, S.T.; Kwok, H.S. 3×3 Matrix for unitary optical systems. J. Opt. Soc. Am. A **2001**, *18*, 2138–2145.

MARCEL DEKKER, INC.
270 Madison Avenue, New York, New York 10016